Application of teleseismic receiver functions and Gravity for Moho depth mapping: A case study of Western Himalayas

Mohammad Salam (salamphysicist@hotmail.com)
Centre for Earthquake Studies (CES), National Centre for Physics (NCP), Islamabad

Jamil Ahmed
Centre for Earthquake Studies (CES), National Centre for Physics (NCP), Islamabad

Waqar Ali Zafar
Centre for Earthquake Studies (CES), National Centre for Physics (NCP), Islamabad

Muhammad Tahir Iqbal
Centre for Earthquake Studies (CES), National Centre for Physics (NCP), Islamabad

Imran Khan
Centre for Earthquake Studies (CES), National Centre for Physics (NCP), Islamabad

Amir Sultan
Centre for Earthquake Studies (CES), National Centre for Physics (NCP), Islamabad

Talat Iqbal
Centre for Earthquake Studies (CES), National Centre for Physics (NCP), Islamabad

Research Article

Keywords: Moho, Himalayas, Pakistan, Receiver Function, H-k Stacking, Crustal Structure, Gravity, Bouguer

Posted Date: August 1st, 2022

DOI: https://doi.org/10.21203/rs.3.rs-1888015/v1

Application of teleseismic receiver functions and Gravity for Moho depth mapping: A case study of Western Himalayas

Mohammad Salam[1*], Jamil Ahmed[1], Waqar Ali Zafar[1,2], Muhammad Tahir Iqbal[1], Imran Khan[1], Amir Sultan[1] and Talat Iqbal[1]

[1*]Centre for Earthquake Studies (CES), National Centre for Physics, Islamabad, Pakistan.
[2]DNE, Pakistan Institute of Engineering and Applied Sciences, Nilore, Islamabad, Pakistan.

*Corresponding author(s). E-mail(s): salamphysicist@hotmail.com;
Contributing authors: jamil.bce@gmail.com; waqaraliravian@gmail.com; tahirgeologist@yahoo.co.uk; emailto.ahmed.bilal@gmail.com; amirsultan_pk@yahoo.com; talat.iqbal@ncp.edu.pk;

Abstract

This study presents the coherently stacked P-wave receiver functions and bouguer anomaly mapping of Western Himalayas (longitude **71°-74°*E*** and latitude **31°-34°*N***) to estimate crustal thickness. Data used for P-wave receiver function is from local seismic network of Pakistan whereas, gravity data is extracted from Topex available in public domain for research. The crust thickness and average crust Vp/Vs ratio at each station of the network is obtained by coherently stacking the Ps, PpPs, PpSs + PsPs phases of 15 seismic stations. The data used in this study was collected from 2012 to 2019, events with magnitudes mb $\geq$ 6 and epicenteral distances **30°** to **95°** were chosen. There is a significant difference in Moho depth beneath the broadband seismic stations used for the investigations.

Moho depth is 36 km in the south, on average 46 km in the center, and 52 km at the northernmost seismic station of the study area. In general, the crust is dipping from South to North for the study area. In order to support this interpreted argument of moho-depth variation from P-Wave receiver function, residual calculation of bouguer anomaly data was carried out as well. The residuals showing a variation of anomalous data from -89 to 193 ***mGal*** in study area have presented a promising correlation and favored the argument of crustal dipping as suggested by P-wave function from seismic network. The trend confirms that the crustal thickening and shortening is caused by the collision of Indian and Asian plates.

Keywords: Moho, Himalayas, Pakistan, Receiver Function, H-k Stacking, Crustal Structure, Gravity, Bouguer

1 Introduction

Western Himalayas which lays in Northern Pakistan is regarded as one of the most appealing locations on the globe by geo-scientific community because of its unique tectonic features, also the country has experienced many devastating earthquakes in history. Northern Pakistan is prone to earthquakes, which occur as a result of the continuing indentation of the strong Indian block into the softer Eurasian block (Tapponnier et al, 1982). As a result, shallow and intermediate-depth earthquakes occur in the Himalayas and Hindukush, respectively (Jackson and Yielding, 1983). According to recent study, the energy stored in the Himalayas increases the likelihood of future earthquakes with $Mw > 8.0$ (Durrani et al, 2005; Stevens and Avouac, 2016). Therefore, investigation of deep structure in this area is critical for understanding tectonic inheritance, history and occurrence of earthquakes.

Thickness of geological interfaces of subsurface varies to a large extent within the sedimentary basins and across the continental boundaries. Mapping these crustal structure variations is critical for understanding the processes of subduction systems, hydrocarbon habitats and continental rift. Subsurface

geological formations can be determined through deep seismic analysis. Teleseismic body-waves encompass a lot of details on the 3-D structure of interior of the Earth as these waves are receptive to the physical properties of the media through which they traveled. It is still an open question, how to extract the most relevant informations about the structure of the earth from these seismograms. Seismic tomography on global level comprehend numerous ways to obtain velocity anomalies from seismic wave traveltime anomalies in the subsurface (Owens et al, 1984). Receiver function method was developed for determination of structural variations in the deep earth, using converted waves generated on discontinuities like Moho, upper mantle discontinuity and bottom boundary of the lithosphere.

A receiver function (RF) is the response of structure of the Earth to an incident teleseismic wave below a seismometer, it consists of a series converted waves from P-to-S or S-to-P generated at structural discontinuity (Langston, 1979). It is mostly used to image major boundaries within the Earth. The Moho interface, is the borderline between the bottom of the crust and the underlying top of the mantle. In Receiver Functions (RFs) P-to-S (Ps), which is Moho-converted phase from an incident P wave, is used to find crustal thickness or Moho depth (H) under a seismic station. Crustal thickness is a vital factor for understanding tectonic evolution and regional geology, but it has a great reciprocity with Vp/Vs ratio (k) in crust. To reduce this trade-off crustal reverberations (multiples) of Ps are used in analysis (Zandt et al, 1995; Zhu, 1993; Zhu and Kanamori, 2000). The H-k stacking method proposed by (Zhu and Kanamori, 2000) with a grid-search algorithm that find out the Vp/Vs ratio and Moho depth (H) with the acquired P-wave RFs at a station, has been commonly used to evaluate the thickness and average Vp/Vs of the crust. In this method the amplitudes of RFs are stacked at the expected arrival times of

Ps and its crustal reverberations (PpPs and PpSs + PsPs) for given values of H and k. This method is pervasive and gives good results, assuming isotropic crust and flat Moho.

The contrasting patterns of gravity data variation in a particular area is caused by difference of the density value of subsurface lithological units. This reliable potential field application is advantageous in terms of time-saving and efficient. In general gravity data gives a regional picture of scanned area (Caku et al, 2020; Han et al, 2020; Li et al, 2010; Zafar et al, 2022). the regionally mapped bouguer anomaly calculated from field gravity data is an expression of the accumulative density contrast from core to crust of the observation site (Sheng et al, 2018; Wei and Yang, 2006; Zafar et al, 2019, 2022). However, in order to amplify the effects of near surface features on gravity data further processing of the data is needed. These impacts can be highlighted using 1st order vertical derivative or the residuals separation from the regional data (Zafar et al, 2019, 2022; Li et al, 2010). This regional to residual separation can be performed by using different tools and filters. The available filter of residual separation in Oasis Montaj GM can be applied with little modification in tolerance and preset band pass level when large data span is being used (Zafar et al, 2022, 2019).

The aim of this study is to compute crustal structure variation in Western Himalayas (longitude 71°-74°E and latitude 31°-34°N) using combination of receiver functions and H-k stacking algorithm and Bouguer anomaly mapping.

2 Study Region

For a geologist, Pakistan is a vast museum of geological formations that change from region to region owing to varying tectonic regimes. The country is located at the intersection of three tectonic plates: Arabian, Indian, and Eurasian.

Pakistan's geology can be divided into four major divisions: The eastern part consisting of Thar Desert and the Indus Plain, Chaman transform plate boundary along the western border, the Hindukush- Himalaya-Pamir continental collision zone in the North, and Makran subduction zone in the South (Kazmi and Jan, 1997). Our study area mainly covers the northern part of Pakistan, which is the most seismically active region being the leading edge of active tectonics (as shown in Figure 1).

The current study area is bounded to the south by Indus Plain and to the north by Himalayan orogenic belt along the northern collision zone. The accumulation of mass along collision zone resulted in the formation of the Himalayas, spanning about 2500 km and forming the Indo-Pakistan plate margin with Eurasia (Le Fort, 1975). The major cause of earthquakes along this collision zone is continental convergence of the Indian and Eurasian plates at a rate of about 40 mm/year, combined with slow anticlockwise rotation (Lisa et al, 2009). About 70Ma, India separated from Gondwanaland and drifted northward with gradual rotation until it collided with the Eurasian Plate in Eocene (Stocklin, 1974; Stoneley, 1974; Molnar, Peter and Tapponnier, Paul, 1975). Main Karakoram Thrust (MKT) is indeed the consequence of deformation that began along the suture zone. The deformation then gradually shifted south away from the collision zone and resulted in formation of Main Mantle Thrust (MMT), eventually reaching the Main Boundary Thrust (MBT) marking the northern extent of current study area. Finally it migrated to the current deformation front along Salt Range Thrust (SRT) and Trans-Indus Ranges Thrust (TIRT) round about 2 M.a; the deformation has been documented to be as young as 0.4 Ma (Le Fort, 1975; Kazmi and Jan, 1997; Yeats and Lawrence, 1984). Instruments bearing numbers S07, S09, S10, S11, S12, S13 and S14 used in the study have been installed along this deformation

front; while, instrument S15 is located on buried Sargodha Cratonic Ridge in the Punjab Plains. This ridge sub-parallel to the deformation front is thought to be formed as foreland bulge due to enormous weight of Himalayan orogen (Abir et al, 2015; Virdi, 1994).

Crust of Pakistan consists of two major parts: 1)- The Indian Shield (also known as Indian Craton) and 2)- thick sedimentary cover. According to seismic and gravimetric studies, the continental crust in the Indian Plate has an average thickness of 30-40 km, thickens beneath the Himalayas up to 60 km, and has a thickness of 80 km beneath the Tibetan Plateau (Le Fort, 1975; Horton et al, 2004; Hetenyi et al, 2006; Unsworth et al, 2005).

3 Data and Method

Centre for Earthquake Studies (CES) is running a network which mostly comprises of broadband digital seismic stations. The majority of these seismic stations are located in northern Pakistan (Western Himalayas), with a few stations installed in the country's central and southern regions. This study was conducted in the northern part of the country, and 15 broadband seismic stations were used for crustal structure analysis, as shown in Figure 1. CMG-3T, CMG-3ESP, and CMG-6TD sensors of Guralp Systems Limited, as well as KS-2000 seismometer from Geotech are in use at CES. The data used in this study was collected from 2012-01-01 to 2019-09-25. Teleseismic events with magnitudes ≥ 6.0 and epicentral distances from 30° to 95° were selected for this study so that the waveforms were not contaminated by strong Upper Mantle or Core waves. From the data bank of CES, on average 110 events per station were obtained out of 226 teleseismic earthquakes data. A more selective approach was used by looking at the recording period length and background

noise level yielding 42 to 94 events for each station, as shown in Table 1. Due to ample epicentral distance and azimuthal coverage, lateral changes even out.

In this study, receiver functions provide us the key information about the crustal structure beneath the station. (Langston, 1979). Time-domain iterative deconvolution technique is employed to compute receiver functions (RFs)(Ligorria and Ammon, 1999). Taup Toolkit is used to compute theoretical arrivals of different phases and cut waveforms in the corresponding time windows for further RF analysis (Crotwell et al, 1999). H-k stacking technique (Zhu and Kanamori, 2000) is used to stack several events coherently to improve signal to noise ratio (SNR). The classification and identification of various Moho converted phases abides by the convention of (Bath and Stefãnsson, 1966). Phases which are entering the layer are named with lowercase letters while those which are leaving the layer are named with uppercase, as depicted in Figure 2. SplitRFLab, a MATLAB toolbox, is used for receiver functions computation and H-k stacking analysis (Wustefeld et al, 2008; Xu et al, 2016).

The H-k method has become a standard seismology technique, leveraging the Ps phase and its crustal multiples PpPs and PpSs + PsPs to resolve the H-k trade-off. For radial RF, equation 1 explains the relation among crustal thickness (H), velocities, time separation between reverberated phases and the direct P phase (Zhu and Kanamori, 2000).

$$\begin{aligned} H &= \frac{t_{Ps}}{\sqrt{\frac{1}{V_s^2} - p^2} - \sqrt{\frac{1}{V_p^2} - p^2}} \\ &= \frac{t_{PpPs}}{\sqrt{\frac{1}{V_s^2} - p^2} - \sqrt{\frac{1}{V_p^2} - p^2}} \\ &= \frac{t_{PpSs+PsPs}}{2\sqrt{\frac{1}{V_s^2} - p^2}} \end{aligned} \tag{1}$$

In this case, p is the incident wave's ray parameter.

$$s(H,k) = \omega_1 r(t_1) + \omega_2 r(t_2) - \omega_3 r(t_3) \tag{2}$$

where t_1, t_2, and t_3 are the predicted arrival times of Ps, PpPs, and PpSs+PsPs of radial receiver functions r(t), and ω_i are the weighting factors such that $\sum \omega_i = 1$. The s(H, k) reaches to the maximum when all three phases are stacked coherently with the appropriate H and Vp/Vs ratio k.

In equation 2 the following weighting factors are used to calculate the receiver functions:

$$\omega_1 = 0.7, \quad \omega_2 = 0.2 \quad and \quad \omega_3 = 0.1$$

The values are selected according to the signal-to-noise ratio of the phases e.g. Ps SNR and weighting factor is more than other two. ω_1 is set greater than $\omega_2 + \omega_3$ because in H-k plane ω_2 and ω_3 have analogous trend. In all of the stacking process, crustal P velocity of 6.3 km/s (average value) is used. The maxima of the 2 yields the crustal thickness and Vp/Vs ratios. Using (Eaton et al, 2006), uncertainties of (Vp/Vs, H) pair were calculated and it is depicted with the ellipse in Figure 3 . Furthermore, RFs are collected against their ray parameters. These RFs are stacked and we get a ray parameter profile of RFs. This gives us the visual view of the predicted arrival times of Ps and multiples.

Firstly, Taup Toolkit is used to compute theoretical arrival times. This is done because accurate P-arrival times are not required for the RF analysis. After that waveforms in an expanded time window containing P-wave phase are chosen. It is observed that the frequency bands of the noise are not the same in all waveforms, RFs are calculated using Butterworth filter of $3rd$ order in three frequency ranges (0.03-2 Hz, 0.06-2 Hz, and 0.1-2 Hz) and then chose

the best result. SNR value of P-wave phase is obtained by comparing the waveforms before the theoretical arrivals and after it and 10s length of waveform is used for this purpose. At start, SNR cut-off values for radial and vertical components are computed. Selected waveforms with SNR greater than the cut-off values are sorted out to compute RFs to get efficient results. The obtained RFs are plotted to check and choose the best result from three different frequency bands as shown in Figure 2.

In addition the Bouguer anomalous pattern in the study region has been implemented to interpret the moho depth variation in this study as an aid to verify the results computed from tele-seismic receiver functions. The data used in the study is acquired from Satellite Geodesy mission of Scripps Institution of Oceanography, University of California, San Diego, a data source available in public domain for research purposes at http://https://topex.ucsd.edu/cgi-bin/get_data.cgi/. The data density found in the study region is found to be at a grid of approximately $1.5x1.5km^2$. In this way a total of 32400 gravity data points were extracted for the said study region. Generally, bouguer anomaly shows pattern of increasing and decreasing with basement rock uplift or subsidence respectively because of moving more denser material towards the ground surface. In this study we filtered the bouguer anomaly data using Gaussian filter for separation of regional to residuals. In order to mark the variations sharply grid-fill method with maximum entropy (Li et al, 2010) is applied along with horizontal and vertical derivatives of the originally grided data as dx and dy respectively. These derivatives have been further combined for both regional and residual grids using following relation (Zafar et al, 2022),

$$G_0 = \sqrt{dx^2 + dy^2} \tag{3}$$

Where, G_0 is final grid of regional as well residual data, dx is the 1^{st} order horizontal derivative of regional as well as residual data, and dy is the 1^{st} order vertical derivative of both regional and residual grids in the upcoming section both regional and residual variations of bouguer anomaly in the study area are discussed.

4 Results and Discussion

4.1 Receiver Function and H-K Stacking

To determine the crustal structure beneath the seismic stations, we used receiver functions and the H-k stacking algorithm. Whereas, the delay times were obtained from the sum trace for each station after the stacking of multiple telesiesmic events. A strong positive (rising edge) signal is present in all the stations data with a delay time after P arrival of 5-6 s, representing the P-to-S converted signal from the Moho discontinuity. The presence of other positive signals with time delays of 15-22 s and negative signals with time delays of 20-29 s, represents multiple reverberations within the crust for the phases PpPs and PpSs+PsPs respectively, as shown in figure 2. The corresponding crustal thickness ranges from 51.9 km below station S01 to 36.2 km below station S15, with a Vp/Vs ratio ranging from 1.61 to 1.83, as shown in table 1 and figure 4.

The Moho depth is shallowing from north to south, and the crustal thickness for seismic stations S01 to S05 ranges from 51.9 to 50.2 km, with an average of 51 km. For stations S06 to S14, the variation in moho depth is small and random; the crustal thickness ranges from 47.1 to 45.1 km, with an average of 46 km. The crustal thickness for S07 and S08 is 45.1 and 45.4 km, respectively, which is lower than the other nearby stations. Variation in surface topography may account for this difference. Station S15 is located on the Sargodha Cratonic Ridge zone, where the Indian shield is exposed to the

surface, resulting in a shallow moho. Based on the results, the selected area can be divided into three sections: Moho is shallow in the south, deeper in the north while moderate in the center.

Comparison with other seismological studies is relatively tough as the structural variations beneath the earth's surface in the Pakistan region are poorly understood due to scarce study in this area. However, some limited study is available for the nearby regions which is geologically significant, and is crucial for understanding the trend and growth of the Himalayas. Aibing and Bongani (2009) performed teleseismic receiver functions analysis to obtain crustal structure in the Pakistan Himalayas and reported 52-53 km of Moho depth in Peshawar basin, which is just in north of our north-most seismic stations S01 and S02. Johnson and Vincent (2002) integrated previous studies and developed a 3-D Velocity model for the Pakistan-India region. They proposed a crustal thickness of 50 km in the northern Pakistan. Vinnik et al (2007), on the other hand, indicate a slightly larger value of crustal thickness by performing joint inversion of P and S receiver functions for the same area. Menke (1977) and Ni et al (1991) both proposed a north-east dipping Moho.

We also compared our results with other geophysical techniques. For example, Rizwan et al (2021) estimated crustal thickness of 51.2-52.6 km using gravity data in the Mansehra-Battal, Haraza ($73 - 73.4^{\circ}E$ and $34.2 - 34.6^{\circ}N$) region of Pakistan. This area is slightly towards north from our north-most seismic station S01. Alexey et al (2018) worked on crustal structure for Tibet and surrounding area using seismic, gravimetric and combined (seismic-gravimetric) Moho model. Their results showed the Moho depth of 38-52 km by seismic, 35-55 km by gravimetric and 37-53 km by seismic-gravimetric, for our study area. Similarly Mehdi et al (2016) used gravity and topographic/bathymetric data for the gravimetric modeling of Moho discontinuity. The

hydrostatic or flexural theories of the isostasy, also suggests discontinuity at a depth of 36-55 km (Mehdi, 2016). Furthermore, Moho density contrast of 35-50 km is reported for the same region using the gravity-gradient data acquired from the Gravity field and steady-state Ocean Circulation Explorer (GOCE) along with the elevation data from the Shuttle Radar Topography Mission (SRTM) and other global datasets (Mehdi et al, 2016). Other regional-scale gravity studies performed in different areas of northern Pakistan with the objectives of delineating crustal structures and flexural rigidity (Caporali, 1995, 2000a,b; Duroy, 1986; Marussi, 1976; Das et al, 1979) reveal a similar trend.

Keeping in view these different geophysical and empirical calculations, we combined our seismic investigations with gravimetric analysis data acquired by Satellite Geodesy mission of Scripps Institution of Oceanography, University of California, San Diego. All these studies suggest that our findings are consistent with the results obtained through other methods for crustal structure variation in the study area. In fore-coming sections we have discussed the findings of gravimetric studies in our area to cross correlate the findings of tele-seismic functions.

4.2 Gravity Implementation

The regional anomaly pattern as suggested from the terminology gives an overall regional pattern of the features causing abnormality in the subsurface. The regional variation plot in 5 suggests existence of some denser material dipping gradually from south to North of the study area. Variation of the anomaly values from -134 to 18 milli gals (mGals) as mentioned in scale of the plot gives insight to further investigate and differentiate the causative feature in subsurface. In the study region geological pattern varies from Punjab plains in south

having an alluvium cover to pothohar and foot hills of Himalayan region in North. The variation in regional map is in accordance with the general geological pattern of the study area. In order to delineate and mark the subsurface features which show the pattern of shortening to deepening of the Moho from south to North of the study area by tele-seismic functions, residual separation with damping factor of 0.2 in Gaussian filter was carried out.

Map in 6 shows the residual plot of the bouguer anomaly as separated from regionals using Gaussian filter. As mentioned in 6 the bouguer anomaly residuals vary from -89 to 193 mGals. This abnormal variation in anomaly values is caused by the near surface features. It is quite evident from 6 that the denser material causing this variation is dipping from South to North of the study area. However, a sharp contrast in anomaly pattern at 32.40 latitude is unusual in the dipping structure in subsurface. In order to mark and investigate this contrasting zone we plotted the prominent tectonic features along-with the residuals of the anomaly. In order to keep maps, tidy we limited these features to SRT, Jhlum and Kalabagh faults only. SRT (Salt Range Thrust) is one of the most studied features in this area by researchers. This thrust is accommodating a good slip being caused by tectonic movement from South to North because of its plasticity. Plot of this thrust in the map mentioned that the sudden and sharp gravity variation is being caused by this feature. The salt dome is offering higher density and shows an increase of anomalous value to maximum in this area i.e up to 193 mGals. The gradual decreasing pattern in gravity values from south to North beyond this structure reaches to minimum of the study region i.e up to -83 mGals.

This variation of the anomaly pattern strengthens the idea of deepening of Moho or the increase in crustal thickness to North of the study area as suggested by the tele-seismic functions.

5 Conclusion

Using CES broadband data, we computed receiver functions and determined the crustal structure variations beneath the seismic stations. The time domain iterative deconvolution algorithm was chosen to compute the RFs, because of its desirable characteristics. The results have been compared with previous RF studies in the neighboring areas and found compatible and verified with other geophysical studies like gravity surveys etc in the same area. The results from the H-k stacking method are more coherent and reliable because Ps and multiples, as well as the Vp/Vs ratio, are used to determine crustal thickness. Aforesaid findings have been cross correlated with the gravity data mapping of the study area. The near surface feature's impact enhancement using residual plot has shown the same dipping phenomenon of Moho as observed by H-k stacking method. In conclusion, this study shows that crustal variation in the central part of the study area is low, with a moderate thickness while crustal thickness is shallower in the south and increases towards north; a slight increase is observed from west to east. In general this study shows a north-east dipping Moho. Moreover, these preliminary results of the study suggest that, combination of these two diverse field observations can be applied for such tectonic feature marking confidently.

Acknowledgments

We would like to thank everyone at Data Management and Instrumentation, CES, for allowing us to use seismic data. We are also grateful to Dr. Mohammad Tahir and Dr. Riaz Ahmad Soomro for their insightful comments on this manuscript. Authors would like to say special thanks to Team Geophysics AEMC, Lahore for helping in Gravity Data Interpretation.

Table 1 Moho depth (H) in Kilometers and Vp/Vs ratios are presented for 15 seismic stations, N RFs represent the number of receiver functions.

Station	**H(km)**	$k = Vp/Vs$	**N RFs**
S01	51.9±0.8	1.75±0.03	86
S02	51.8±0.5	1.72±0.05	90
S03	51.9±0.9	1.75±0.04	84
S04	51.1±0.4	1.72±0.02	79
S05	50.2±0.8	1.72±0.05	94
S06	47.1±0.6	1.61±0.03	74
S07	45.1±1.2	1.61±0.04	62
S08	45.4±0.9	1.63±0.05	86
S09	46.4±0.5	1.77±0.03	88
S10	46.8±0.9	1.83±0.04	74
S11	46.9±0.5	1.66±0.05	65
S12	46.8±0.7	1.70±0.05	47
S13	46.5±0.6	1.82±0.03	42
S14	45.1±1.1	1.77±0.04	88
S15	36.2±0.9	1.78±0.05	48

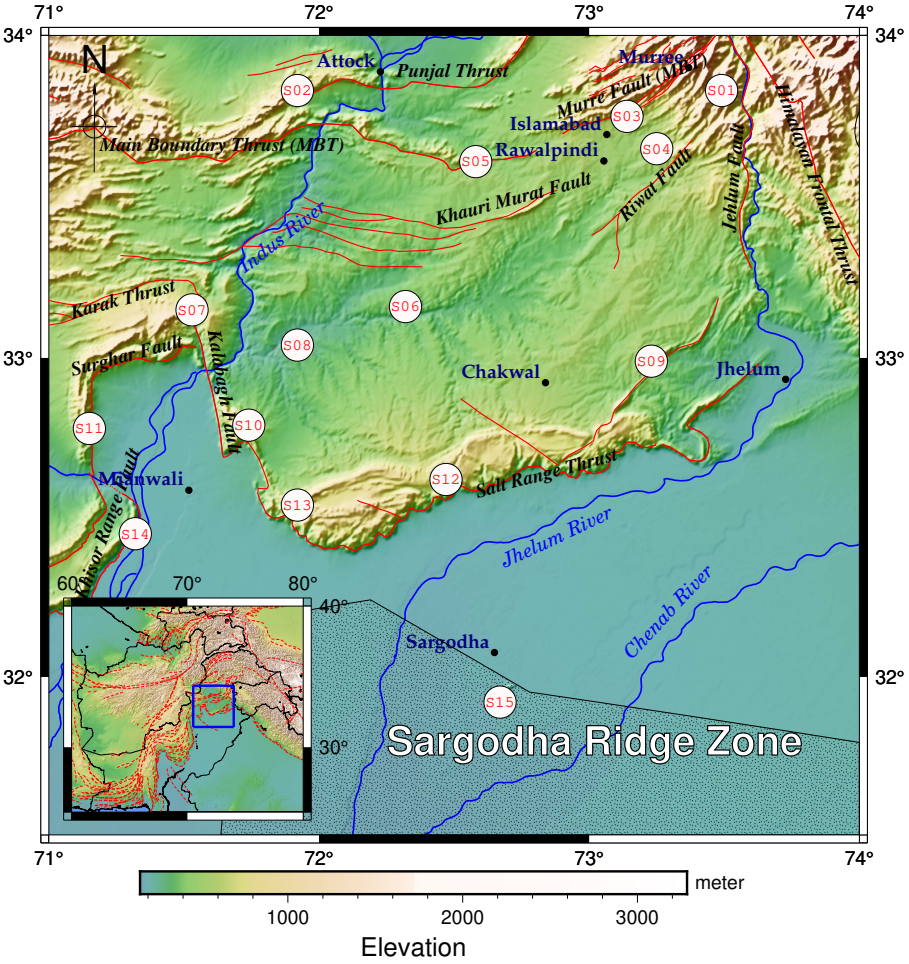

Fig. 1 Seismic network of CES is displayed over topographic relief and fault lines of the study area, modified from (Kazmi and Rana, 1982). Stations name within the circle represent broadband three component seismic station, used in this study.

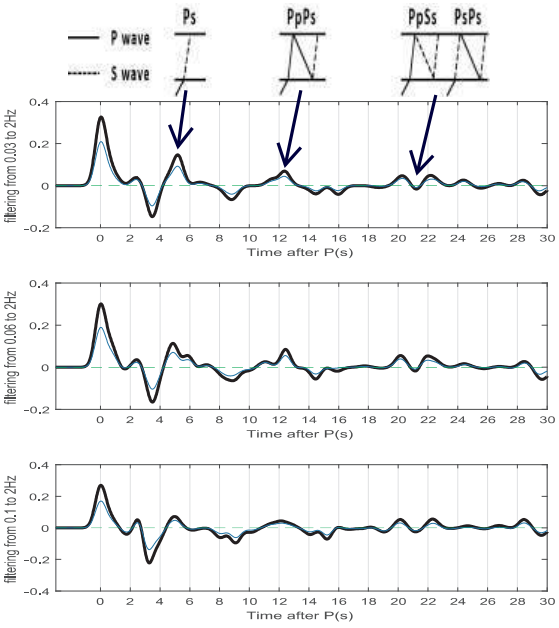

Fig. 2 The Moho converted phase Ps, the largest peak just after P wave arrival and the multiples PpPs, and PpSs+PsPs are labeled, and their ray paths are illustrated at the top. A 3^{rd} order Butterworth filter in three different frequency bands (0.03-2 Hz, 0.06-2 Hz, and 0.1-2 Hz) is applied. The classification and identification of various Moho converted phases abides by the convention of (Bath and Stefánsson, 1966). Phases which are entering the layer are named with lowercase letters (except for the first arrival) while those which are leaving the layer are named with uppercase.

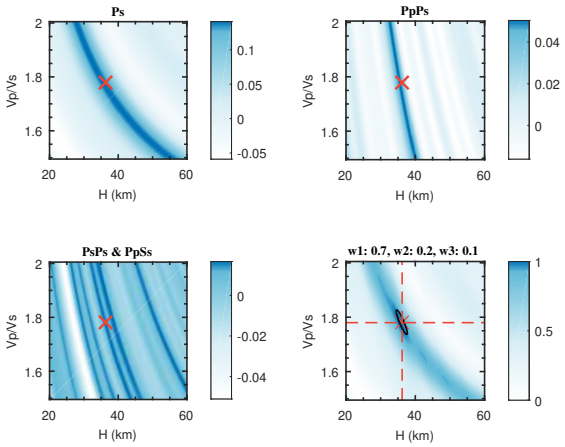

Fig. 3 H-k domain $s(H,k)$ for Ps (TL), PpPs (TR), PsPs+PpPs (BL) and the cumulative of all three (BR), with $\omega_1 = 0.7, \omega_2 = 0.2$ and $\omega_3 = 0.1$ for station S15. The $s(H,k)$, best estimate of the crustal thickness is 36.2±0.9 km and Vp/Vs ratio of 1.78±0.05. The 1σ uncertainties are given by the ellipse.

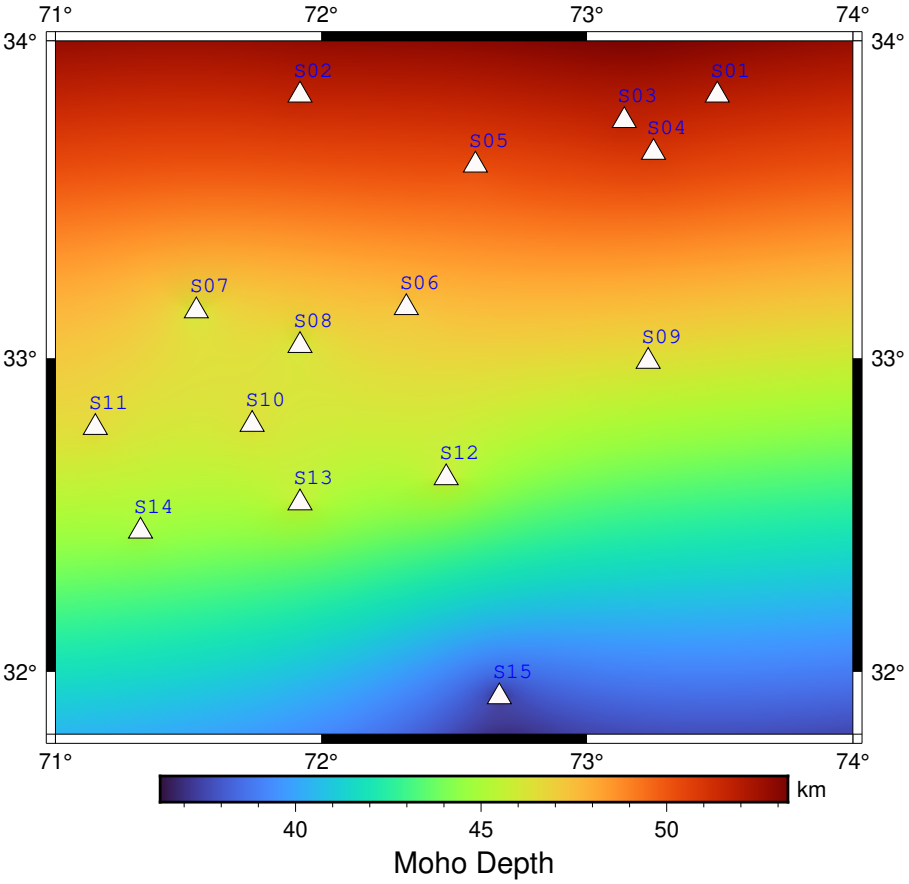

Fig. 4 Map of the Moho depth for Western Himalayas. Moho is shallow in south and increases towards north, a slight increase is also observed from west to east. Overall it is a north-east dipping Moho.

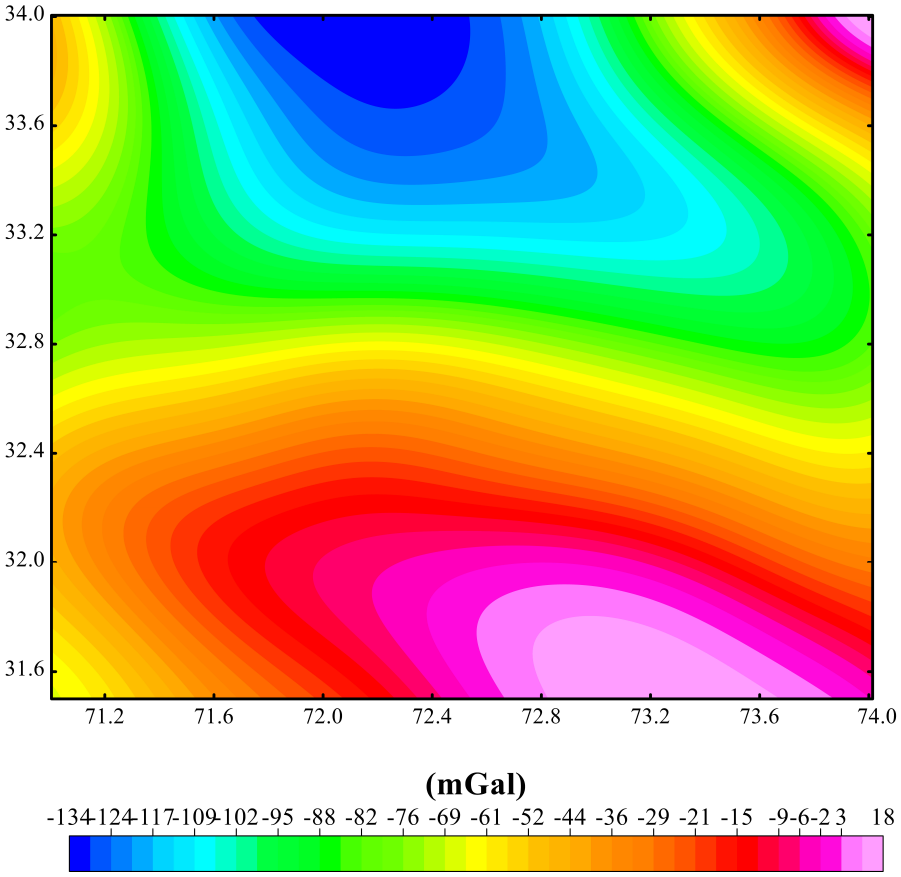

Fig. 5 Regional bouguer anomalous pattern in the study area as derived after application of the filters mentioned above.

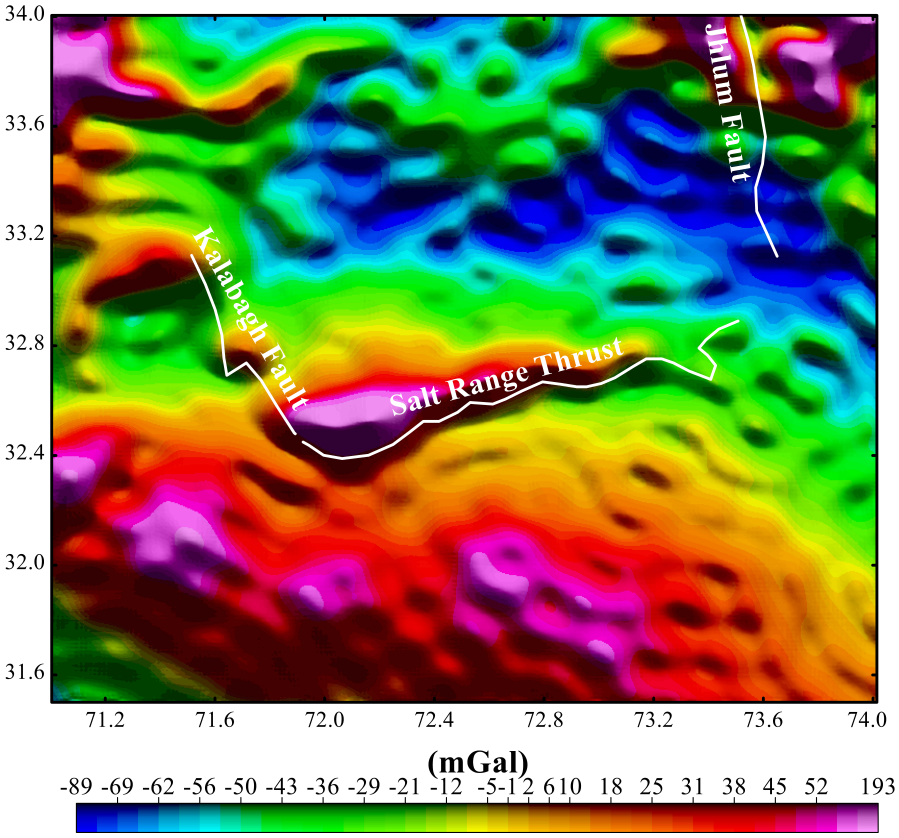

Fig. 6 Residual bouguer anomaly plot of the study area. showing enhanced effects of the near surface features along with prominent tectonic structures in the study area.

References

Abir IA, Khan SD, Ghulam A, et al (2015) Active tectonics of western 319 potwar plateau–salt range, northern pakistan from insar observations and seismic imaging. Remote 320 Sens Environ 168

Aibing L, Bongani M (2009) Crustal structure in the pakistan himalaya from teleseismic receiver functions. Geochemistry Geophysics Geosystems

Alexey B, Mohammad B, Robert T (2018) Combined gravimetric-seismic moho model of tibet. Geosciences

Bath M, Stefãnsson R (1966) SP conversion at the base of the crust. Annals of Geophysics 19:119–130

Caku N, Gwavava O, Liu K, et al (2020) An integration of magnetic, gravity and seismic data in evaluating the algoa basin in the eastern cape province of south africa for stratigraphic and structural geodynamics. Pure and Applied Geophysics 177(9):4177–4205

Caporali A (1995) Gravity anomalies and the flexure of the lithosphere in the karakoram, pakistan. J Geophys Res Solid Earth

Caporali A (2000a) Buckling of the lithosphere in western himalaya: constraints from gravity and topography data. J Geophys Res Solid Earth

Caporali A (2000b) The gravity field of the karakoram mountain range and surrounding areas. Geol Soc London, Spec Publ 170:7–23

Crotwell HP, Owens TJ, Ritsema J (1999) The TauP Toolkit: Flexible seismic travel-time and ray-path utilities. Seismological Research Letters 70(2):154–160

413 Das D, Kgc R, Al R (1979) Bouguer, free-air and magnetic anomalies over
414 north-western himalayas.

415 Duroy Y (1986) Subsurface densities and lithospheric flexure of the himalayan
416 foreland in pakistan interpreted from gravity.

417 Durrani AJ, Elnashai AS, Hashash Y, et al (2005) The kashmir earthquake of
418 october 8, 2005: A quick look report. MAE Center CD Release 05-04

419 Eaton DW, Dineva S, Mereu R (2006) Crustal thickness and Vp/Vs varia-
420 tions in the Grenville orogen (Ontario, Canada) from analysis of teleseismic
421 receiver functions. Tectonophysics 420:223–238

422 Han R, Li W, Cheng R, et al (2020) 3d high-precision tunnel gravity explo-
423 ration theory and its application for concealed inclined high-density ore
424 deposits. Journal of Applied Geophysics 180:104,119

425 Hetenyi G, Cattin R, Vergne J, et al (2006) Mesozoic-cenozoic evolution
426 of the xining-minhe and dangchang basins, northeastern tibetan plateau:
427 Magnetostratigraphic and biostratigraphic results. Journal of Geophysical
428 Research: Solid Earth

429 Horton BK, Dupont-Nivet G, Zhou J, et al (2004) Mesozoic-cenozoic evolution
430 of the xining-minhe and dangchang basins, northeastern tibetan plateau:
431 Magnetostratigraphic and biostratigraphic results. Journal of Geophysical
432 Research: Solid Earth

433 Jackson J, Yielding G (1983) The seismicity of Kohistan, Pakistan: source
434 studies of the Hamran (1972.9. 3), Darel (1981.9. 12) and Patan (1974.12.
435 28) earthquakes. Tectonophysics 91(1-2):15–28

436 Johnson M, Vincent C (2002) Development and testing of a 3d velocity model
437 for improved event location: A case study for the India-Pakistan region.
438 Bulletin of the Seismological Society of America 92:2893–2910

439 Kazmi AH, Jan MQ (1997) Geology and tectonics of Pakistan. Graphic
440 publishers

441 Kazmi AH, Rana RA (1982) Tectonic map of Pakistan, 1:2,000,000. Geological
442 Survey of Pakistan, Quetta

443 Langston CA (1979) Structure under mount rainier, washington, inferred
444 from teleseismic body waves. Journal of Geophysical Research: Solid Earth
445 84:4749–4762

446 Le Fort P (1975) Himalayas: the collided range. Present knowledge of the
447 continental arc. Am J Sci 275(1):1–44

448 Li SL, Meng XH, Guo LH, et al (2010) Gravity and magnetic anomalies field
449 characteristics in the south china sea and its application for interpretation
450 of igneous rocks. Applied geophysics 7(4):295–305

451 Ligorria JP, Ammon CJ (1999) Iterative deconvolution and receiver-function
452 estimation. Bulletin of the SeismologicalSociety of America 89:1395–1400

453 Lisa M, Khwaja AA, Qasim Jan M, et al (2009) New data on the Indus Kohis-
454 tan seismic zone and its extension into the Hazara-Kashmir Syntaxis, NW
455 Himalayas of Pakistan. Journal of seismology 13(3):339–361

456 Marussi A (1976) The tectonic scheme of central asia (compiled), bouguer
457 anomaly map (1975). Accad Naz Lincei

458 Mehdi E (2016) On vening meinesz-moritz and flexural theories of isostasy and
459 their comparison over tibet plateau. J Geod Sci

460 Mehdi E, Matloob H, Robert T, et al (2016) Moho density contrast in central
461 eurasia from goce gravity gradients. Remote Sensing

462 Menke W (1977) Lateral inhomogeneities in p velocity under the tarbela array
463 of the lesser himalayas of pakistan. Bulletin of the SeismologicalSociety of
464 America

465 Molnar, Peter and Tapponnier, Paul (1975) Cenozoic tectonics of asia: effects
466 of a continental collision. Science 189:419–426

467 Ni JF, Ibenbrahim A, Roecker SW (1991) Threedimensional velocity structure
468 and hypocenters of earthquakes beneath the hazara arc, pakistan: Geometry
469 of the underthrusting indian plate. J Geophys Res

470 Owens TJ, Zandt G, Taylor SR (1984) Seismic evidence for an ancient rift
471 beneath the Cumberland Plateau, Tennessee: A detailed analysis of broad-
472 band teleseismic P waveforms. Journal of Geophysical Research: Solid Earth
473 89:7783–7795

474 Rizwan ASarwar, Ashar K, Chenglin L, et al (2021) Subsurface geological
475 model of sedimentary and metasedimentary wedge from mansehra to battal
476 based on gravity data, hazara area, pakistan. Energy Geoscience

477 Sheng Z, Xiaohong M, Minghua Z, et al (2018) The improved residual node
478 density based gravity forward method and its application. Journal of Applied
479 Geophysics 159:765–772

480 Stevens V, Avouac JP (2016) Millenary mw¿ 9.0 earthquakes required by
481 geodetic strain in the himalaya. Geophysical Research Letters

482 Stocklin J (1974) Possible ancient continental margin in iran; in c. l. drake
483 and c.a.bruke, eds., the geology of continental margins. New York, Springer-
484 Verlag

485 Stoneley R (1974) Evolution of the continental margin bounding a former
486 tethys, in c. l. drake and c. a. burke, eds., the geology of continental margins.
487 New York, Springer-Verlag

488 Tapponnier P, Peltzer G, Le Dain A, et al (1982) Propagating extrusion tecton-
489 ics in Asia: New insights from simple experiments with plasticine. Geology
490 10:611–616

491 Unsworth M, Jones AG, Wei W, et al (2005) Crustal rheology of the himalaya
492 and southern tibet inferred from magnetotelluric data. Nature

493 Vinnik L, Singh A, Kiselev S, et al (2007) Upper mantle beneath foothills of
494 the western Himalaya: subducted lithospheric slab or a keel of the Indian
495 shield? Geophysical Journal International 171:1162–1171

496 Virdi N (1994) The floor of the tertiary basin of northwest india-control of
497 basement highs and 513 palaeotopography on the basin evolution. Remote
498 320 Sens Environ 15

499 Wei Y, Yang Z (2006) The application of combined gravity and seismic
500 data formation separation for revealing deep structure. Applied Geophysics
501 3(4):255–259

Wustefeld A, Bokelmann G, Zaroli C, et al (2008) SplitLab: A shear-wave splitting environment in Matlab. Computers & Geosciences 34:515–528. https://doi.org/10.1016/j.cageo.2007.08.002, URL https://linkinghub.elsevier.com/retrieve/pii/S0098300407001859

Xu M, Huang H, Huang Z, et al (2016) SplitRFLab: A MATLAB GUI toolbox for receiver function analysis based on SplitLab. Earthq Sci 29:17–26. https://doi.org/10.1007/s11589-016-0141-8, URL http://link.springer.com/10.1007/s11589-016-0141-8

Yeats R, Lawrence R (1984) Tectonics of the Himalayan thrust belt in northern Pakistan, Marine geology and oceanography of Arabian Sea and coastal Pakistan BU Haq, JD Milliman, 177–198

Zafar WA, Shakir U, Ahmed J, et al (2019) Application of gravity and radon studies to delineate the concealed section of the khisor thrust. Pure and Applied Geophysics 176(6):2543–2555

Zafar WA, Shakir U, Ahmed R, et al (2022) Gravity and electrical resistivity investigations to mark concealed seepage sources from kanjoor dam, pakistan. Arabian Journal of Geosciences 15(2):1–9

Zandt G, Myers SC, Wallace TC (1995) Crust and mantle structure across the Basin and Range-Colorado Plateau boundary at 37 N latitude and implications for Cenozoic extensional mechanism. Journal of Geophysical Research: Solid Earth 100:10,529–10,548

Zhu L (1993) Estimation of crustal thickness and Vp/Vs ratio beneath the Tibetan Plateau from teleseismic converted waves. Eos Trans AGU 74

525 Zhu L, Kanamori H (2000) Moho depth variation in southern California from
526 teleseismic receiver functions. J Geophys Res 105(B2):2969–2980